Inorganic Chemistry
Communication

Inorg. Chem. **2010**, *49*, 4391–4393 **4391**
DOI: 10.1021/ic100176d

Synthesis of Nanosheet Crystallites of Ruthenate with an α-$NaFeO_2$-Related Structure and Its Electrochemical Supercapacitor Property

Katsutoshi Fukuda,[†] Takahiro Saida,[‡] Jun Sato,[‡] Mihoko Yonezawa,[‡] Yoshio Takasu,[‡] and Wataru Sugimoto*[,†,‡]

[†]*Collaborative Innovation Center for Nanotech Fiber, Shinshu University, 3-15-1 Tokida, Ueda, Nagano 386-8567, Japan, and* [‡]*Faculty of Textile Science and Technology, Shinshu University, 3-15-1 Tokida, Ueda, Nagano 386-8567, Japan*

Received January 29, 2010

Unilamellar crystallites of conductive ruthenium oxide having a thickness of about 1 nm were obtained via elemental exfoliation of a protonic layered ruthenate, $H_{0.2}RuO_2 \cdot 0.5H_2O$, with an α-$NaFeO_2$-related crystal structure. The obtained RuO_2 nanosheets possessed a well-defined crystalline structure with a hexagonal symmetry, reflecting the crystal structure of the parent material. The restacked RuO_2 nanosheets exhibited a high pseudocapacitance of ∼700 F g^{-1} in an acidic electrolyte, which is almost double the value of the nonexfoliated layered protonated ruthenate.

Exfoliation of layered compounds, including clay minerals,[1] metal oxides[2,3] and graphite,[4−7] into two-dimensional (2D) nanosheet crystallites represents a method to obtain a unique class of nanostructured materials.[8] Such low-dimensional nanosheets have promising physicochemical properties associated with the atomic scale thickness and can be used as building blocks to fabricate a variety of three-dimensional architectures with tailored morphology, composition, and porosity.[9] The introduction of nanosheets derived from electroconductive graphite and layered ruthenate has triggered the realization of applications of highly electroconductive nanosheets toward energy-related applications, e.g. supercapacitors,[3,5] fuel cells,[6] and solar cells.[7]

We have especially focused on the synthesis and application of electroconductive $[Ru^{4+}O_{2.1}]^{0.2-}$ nanosheets derived from layered $K_{0.2}RuO_{2.1}$. The water-swellable interlayer space of restacked $RuO_{2.1}$ nanosheets can be utilized for electrochemical charge storage, leading to capacitance as high as 660 F g^{-1}.[3] More recently, Vivekchand and co-workers reported that an exfoliation process in a graphite system also boosts the electrochemical capacitance.[5] As a result of better availability of the graphene surface, reassembled graphene electrodes exhibited enhanced specific capacitance of ∼100 F g^{-1} compared to bulk graphite. Thus, the exfoliation technique can be taken as an effective method in developing practical electrodes for electrochemical storage. Further exploration of highly conductive and supercapacitive nanosheets is still worth investigating. Here, we report a new conductive nanosheet derived from layered sodium ruthenate, $NaRuO_2$, isostructural with α-$NaFeO_2$ and highlight its electrochemical supercapacitor property.

X-ray diffraction (XRD) data of a sample synthesized by a solid-state reaction by heating a mixture of Na_2CO_3:Ru:RuO_2 = 2:1:3 under an argon flow could be indexed based on a hexagonal unit cell with the relationship of $-h + k + l = 3n$, indicating a primitive rhombohedral symmetry (Figures 1a and S1 in the Supporting Information). The refined unit cell parameters, a = 0.30393(5) nm and c = 1.6415(2) nm, are in agreement with those reported for $NaRuO_2$.[10] Traces of unreacted ruthenium was detected as a minor impurity phase. $NaRuO_2$ was treated with aqueous $Na_2S_2O_8$ for oxidative deintercalation of Na ions from the interlayer gallery. Chemical analysis revealed ∼80% removal of Na ions from

*To whom correspondence should be addressed. E-mail: wsugi@shinshu-u.ac.jp. Fax: +81-268-21-5452.

(1) (a) Walker, G. F. *Nature* **1960**, *187*, 312. (b) Nadeau, P. H.; Wilson, M. J.; McHardy, W. J.; Tait, J. M. *Science* **1984**, *225*, 923.
(2) (a) Treacy, M. M. J.; Rice, S. B.; Jacobson, A. J.; Lewandowski, J. T. *Chem. Mater.* **1990**, *2*, 279. (b) Sasaki, T.; Watanabe, M.; Hashizume, H.; Yamada, H.; Nakazawa, H. *J. Am. Chem. Soc.* **1996**, *118*, 8329. (c) Liu, Z.-H.; Ooi, K.; Kanoh, H.; Tang, W.-P.; Tomida, T. *Langmuir* **2000**, *16*, 4154. (d) Schaak, R. E.; Mallouk, T. E. *Chem. Commun.* **2002**, 706. (e) Fukuda, K.; Nakai, I.; Ebina, Y.; Ma, R.; Sasaki, T. *Inorg. Chem.* **2007**, *46*, 4787.
(3) (a) Sugimoto, W.; Iwata, H.; Yasunaga, Y.; Murakami, Y.; Takasu, Y. *Angew. Chem., Int. Ed.* **2003**, *42*, 4092. (b) Sugimoto, W.; Iwata, H.; Murakami, Y.; Takasu, Y. *J. Electrochem. Soc.* **2004**, *151*, A1181. (c) Sugimoto, W.; Iwata, H.; Yokoshima, K.; Murakami, Y.; Takasu, Y. *J. Phys. Chem. B* **2005**, *109*, 7330.
(4) (a) Novoselov, K. S.; Geim, A. K.; Morozov, S. V.; Jiang, D.; Zhang, Y.; Dubonos, S. V.; Grigorieva, I. V.; Firsov, A. A. *Science* **2004**, *306*, 666. (b) Stankovich, S.; Dikin, D. A.; Dommett, G. H. B.; Kohlhaas, K. M.; Zimney, E. J.; Stach, E. A.; Piner, R. D.; Nguyen, S. T.; Ruoff, R. S. *Nature* **2006**, *442*, 282.
(5) Vivekchand, S. R. C.; Rout, C. S.; Subrahmanyam, K. S.; Govindaraj, A.; Rao, C. N. R. *J. Chem. Sci.* **2008**, *120*, 9.
(6) (a) Sugimoto, W.; Saida, T.; Takasu, Y. *Electrochem. Commun.* **2006**, *8*, 411. (b) Si, Y.; Samulski, E. T. *Chem. Mater.* **2008**, *20*, 6792. (c) Seger, B.; Kamat, P. V. *J. Phys. Chem. C* **2009**, *113*, 7990.
(7) Wang, X.; Zhi, L.; Müllen, K. *Nano Lett.* **2008**, *8*, 323.
(8) Jacobson, A. J. *Comprehensive Supramolecular Chemistry*; Alberti, G., Bein, T., Eds.; Pergamon: New York, 1996; Vol. *7*, pp 315−335.
(9) (a) Kaschak, D. M.; Lean, J. T.; Waraksa, C. C.; Saupe, G. B.; Usami, H.; Mallouk, T. E. *J. Am. Chem. Soc.* **1999**, *121*, 3435. (b) Wang, L. Z.; Sasaki, T.; Ebina, Y.; Kurashima, K.; Watanabe, M. *Chem. Mater.* **2002**, *14*, 4827. (c) Muramatsu, M.; Akatsuka, K.; Ebina, Y.; Wang, K.; Sasaki, T.; Ishida, T.; Haga, M. *Langmuir* **2005**, *21*, 6590.
(10) Shikano, M.; Delmas, C.; Darriet, J. *Inorg. Chem.* **2004**, *43*, 1214.

Published on Web 04/21/2010

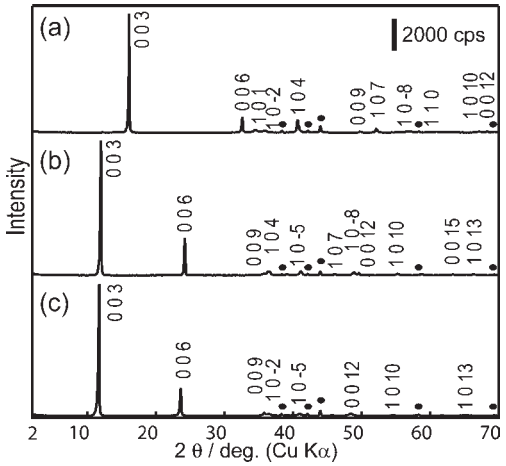

Figure 1. XRD patterns for (a) $NaRuO_2$, (b) an oxidized derivative of that in part a, and (c) a protonated derivative of that in part b. Black circles show peaks due to ruthenium metal.

the interlayer. The oxidized sample retains the characteristic lamellar morphology (Figure S2 in the Supporting Information) and crystallinity of the parent material, indicating that the reaction is topotactic (Figure 1b). The XRD pattern of the oxidized sample could be indexed based on a hexagonal symmetry with $a = 0.29154(7)$ nm and $c = 2.2014(3)$ nm. The values are consistent with those of $Na_{0.22}RuO_2 \cdot 0.45H_2O$ prepared by the reaction of $NaRuO_2$ with H_2O.[10] The decrease in the a axis is attributed to the oxidation of Ru^{3+} to Ru^{4+} in RuO_6 octahedra. The expansion of the c axis can be explained by the smaller charge density of the ruthenate slab due to extraction of Na^+ as well as insertion of water molecules into the interlayer gallery.

Proton exchange of the interlayer Na^+ was attempted by the reaction of the oxidized layered sodium ruthenate with a 1 mol dm^{-3} HCl solution for 48 h. A small shift in the series of basal-plane diffraction peaks to lower angles was observed as a result of proton exchange (Figure 1c). The refined parameters of the acid-treated product were $a = 0.2919(2)$ nm and $c = 2.249(1)$ nm in the hexagonal unit cell, suggesting that the crystal system remains unchanged. Chemical analysis revealed no evidence of residual Na^+ after acid treatment; thus, the acid-treated product can be approximately formulated as $H_{0.2}Ru^{3.8+}O_2 \cdot 0.5H_2O$ (Figure S3 in the Supporting Information). This new compound is the first example of a mixed-valence layered ruthenic acid with cation-exchange capability, being different from $H_{0.2}Ru^{4+}O_{2.1} \cdot 0.9H_2O$ whose Ru ions are tetravalent.[3] The crystallographic data for this compound are summarized in Figure S4 in the Supporting Information.

$H_{0.2}RuO_2 \cdot 0.5H_2O$ was added to an aqueous tetrabutylammonium hydroxide (TBAOH) solution at ambient temperature and shaken for 10 days to initiate exfoliation. The solution-to-solid ratio was adjusted to $TBA^+/H^+ = 0.1, 1, 5, 10, 20$, and 30, where H^+ is the ion-exchangeable proton in the solid. At $TBA^+/H^+ < 1$, powdery deposits can be identified on the bottom of the reaction vessel once the shaking is stopped and the vessel is allowed to stand. Stable colloidal suspensions with dark-green color and a small amount of sediment were obtained at $TBA^+/H^+ \geq 1$. In this region, the volume of the sediments increases with increasing TBA^+/H^+. The sediments could be easily separated from the colloidal suspension by centrifugation at 2000 rpm for 30 min, yielding a considerable amount of a green-black colloid. XRD analysis of a film obtained by casting of the colloid obtained at $TBA^+/H^+ = 10$ exhibited a series of strong diffraction peaks typical of lamellar ordering with $d = 1.65$ nm (Figure 2). The basal spacing suggests that the cast film is composed of an intercalation compound with hydrated TBA^+ (the molecular size of TBA^+ is ~0.9 nm[11]) interleaved between RuO_2 slabs. Note that there is no diffraction peak assignable to ruthenium metal in the pattern because this impurity phase is centrifugally separated as the sediment.

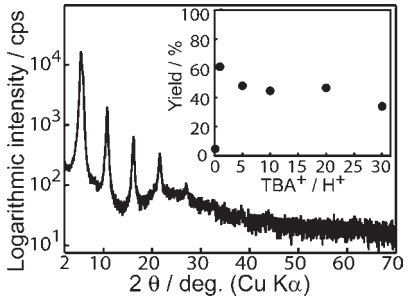

Figure 2. XRD pattern for a thin film obtained by casting of the nanosheet suspension after removal of nonexfoliated materials via centrifugation at 2000 rpm. Inset: plot of the yield of the suspension against the TBA^+/H^+ ratio.

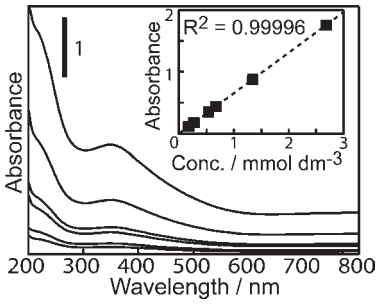

Figure 3. UV−vis absorption spectra obtained from the colloidal suspension of the ruthenate nanosheets with various concentrations. Inset: plot of the absorbance at 350 nm against the concentration of a diluted suspension.

Figure 3 shows optical absorption spectra for ruthenate suspensions with different concentrations. The colloidal ruthenate exhibited a broad peak at a wavelength of 350 nm and an intense absorbance below a wavelength of 250 nm. As a typical example, the absorbance at 350 nm is proportional to the concentration, which is strong evidence that the layered protonic ruthenate is delaminated into monodispersed fragments, i.e., totally exfoliated nanosheets. The molar extinction coefficient for the dispersed nanosheets was estimated to be 6.6×10^3 mol^{-1} dm^3 cm^{-1} at 350 nm.

The nanosheet yield was analyzed by measuring the mass of the exfoliated nanosheet in the supernatant after centrifugation. The nanosheet suspension was completely dried and subsequently heated at 550 °C to remove water and organic compounds and convert the material to anhydrous RuO_2. The highest yield is obtained at $TBA^+/H^+ = 1$ with a yield of ~60% (see Figure 2, inset).

(11) (a) Gao, Q.; Giraldo, O.; Tong, W.; Suib, S. L. *Chem. Mater.* **2001**, *13*, 778. (b) Omomo, Y.; Sasaki, T.; Wang, L. Z.; Watanabe, M. *J. Am. Chem. Soc.* **2003**, *125*, 3568.

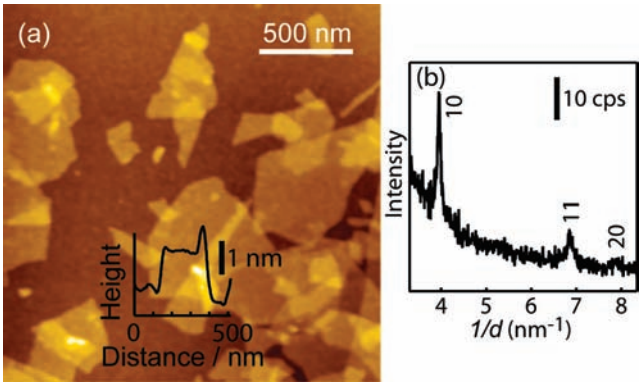

Figure 4. (a) AFM image and (b) synchrotron-radiated in-plane XRD pattern of a RuO_2 nanosheet submonolayer film. Inset in the left panel: height profile along the abscissa.

A diluted nanosheet colloid was directly dropped on a silicon substrate in order to observe the morphology of individual RuO_2 nanosheets by atomic force microscopy (AFM). The AFM images revealed sheets with a thickness of ~1.3 nm and a lateral size ranging from submicrometer to micrometer (Figure 4a). The sheet thickness is reasonable considering the nanosheet structure deduced from the crystallographic data of $NaRuO_2$.[10] The vertical thickness of the host layer is 0.23 nm, and summing up the ionic radius of the two apical oxygen atoms (0.28 nm) gives 0.51 nm. As is often the case with other oxide nanosheets, the difference between the experimental height and crystallographic thickness may be explained by charge-compensating cationic species adsorbed on the nanosheet surface.[11b,12]

In-plane synchrotron-radiated XRD measurement was conducted to gain information on the crystal structure of the RuO_2 nanosheet. A submonolayer film of RuO_2 nanosheets was prepared by a self-assembly technique, where the nanosheets lie parallel to the substrate. All of the observable peaks in the $1/d$ region can be assignable to *hk* reflections of a 2D hexagonal cell (Figure 4b). The refined cell parameter $a = 0.2929(6)$ nm was similar to the *a* axis of the precursor, $H_{0.2}RuO_2 \cdot 0.5H_2O$. This definitely indicates that the 2D atomic arrangement in the original host structure was preserved after the delamination process.

Figure 5 compares cyclic voltammograms of the nonexfoliated, protonated layered ruthenates and the restacked $[Ru^{3.8+}O_2]^{0.2-}$ nanosheets in 0.5 M H_2SO_4 (25 °C). The nonexfoliated material exhibited a specific capacitance of ~420 F (g of RuO_2)$^{-1}$ at 2 mV s^{-1} with a large contribution from charge transfer due to surface redox processes at 0.65 V. The restacked RuO_2 nanosheet electrode exhibited a large

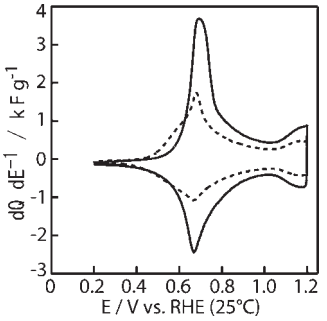

Figure 5. Cyclic voltammograms (potential vs differential capacitance) of protonated layered ruthenates (broken line) and restacked compounds of the nanosheets (solid line) at 2 mV s^{-1} in 0.5 M H_2SO_4.

enhancement in the redox-related charge, leading to a specific capacitance of ~700 F (g of RuO_2)$^{-1}$. The enhancement in the specific capacitance can be understood by construction of a more open framework beneficial to electrochemical charge storage in the restacked RuO_2 nanosheets. The specific capacitance of the restacked RuO_2 nanosheet electrode is comparable to the capacitance of hydrous RuO_2,[13] which is one of the state-of-the-art high-capacitance materials.

In conclusion, we have succeeded for the first time in the preparation and characterization of $[Ru^{3.8+}O_2]^{0.2-}$ nanosheets with well-defined hexagonal symmetry via the soft-chemical delamination of an α-$NaFeO_2$-related layered ruthenium oxide. The specific capacitance is slightly larger than that of $[Ru^{4+}O_{2.1}]^{0.2-}$ nanosheets[3] having a 2D oblique cell[14] and comparable to that of hydrous RuO_2 nanoparticles prepared by sol−gel methods.[13a] The resulting unilamellar crystallites may be useful in a range of applications including microsize supercapacitors, cocatalysts for fuel cells, transparent conducting electrodes, etc.

Acknowledgment. This work was supported, in part, by a "Creation of Innovation Centers for Advanced Interdisciplinary Research Areas" Project in Special Coordination Funds for Promoting Science and Technology of the Ministry of Education, Culture, Sports, Science and Technology, Japan, and CREST of the Japan Science and Technology Agency (JST).

Supporting Information Available: Experimental procedures, XRD patterns, scanning electron microscopy images, a thermogravimetric analysis curve, and crystallographic data. This material is available free of charge via the Internet at http://pubs.acs.org.

(12) Sasaki, T.; Ebina, Y.; Kitami, Y.; Watanabe, M.; Oikawa, T. *J. Phys. Chem. B* **2001**, *105*, 6116.

(13) (a) Zheng, J. P.; Jow, T. R. *J. Electrochem. Soc.* **1995**, *142*, L6. (b) Dmowski, W.; Egami, T.; Swider-Lyons, K. E.; Love, C. T.; Rolison, D. R. *J. Phys. Chem. B* **2002**, *106*, 12677.

(14) Fukuda, K.; Kato, H.; Sato, J.; Sugimoto, W.; Takasu, Y. *J. Solid State Chem.* **2009**, *182*, 2997.